Energy 284 (2023) 128524

Contents lists available at ScienceDirect

Energy

journal homepage: www.elsevier.com/locate/energy

Recovery of chemical energy from retentates from cascade membrane filtration of hydrothermal carbonisation effluent

Agnieszka Urbanowska [a,**], Lukasz Niedzwiecki [b,c,*], Mateusz Wnukowski [b], Christian Aragon-Briceño [d,e], Małgorzata Kabsch-Korbutowicz [a], Marcin Baranowski [b], Michał Czerep [b], Przemysław Seruga [f,g], Halina Pawlak-Kruczek [b], Eddy Bramer [d], Gerrit Brem [d], Artur Pożarlik [d]

[a] Wroclaw University of Science and Technology, Faculty of Environmental Engineering, Department of Environment Protection Engineering, Wybrzeze Wyspianskiego 27, 50-370 Wroclaw, Poland
[b] Wroclaw University of Science and Technology, Faculty of Mechanical and Power Engineering, Department of Energy Conversion Engineering, Wybrzeze Wyspianskiego 27, 50-370 Wroclaw, Poland
[c] Energy Research Centre, Centre for Energy and Environmental Technologies, VSB—Technical University of Ostrava, 17. Listopadu 2172/15, 708 00 Ostrava, Czech Republic
[d] University of Twente, Department of Thermal and Fluid Engineering, Drienerlolaan 5, 7522 NB, Enschede, the Netherlands
[e] Fundacion Circe, Parque Empresarial Dinamiza, Avda. Ranillas 3D, 1ª Planta, 50018 Zaragoza, Spain
[f] Zaklad Gospodarowania Odpadami Gac Sp. Z o.o; 55-200 Olawa, Gac 90; Poland
[g] Wroclaw University of Economics and Business, Department of Bioprocess Engineering, Komandorska 118/120, 53-345 Wroclaw, Poland

ARTICLE INFO

Handling Editor: Wojciech Stanek

Keywords:
Digestate
Hydrothermal carbonisation
Nanofiltration
Biomethane potential
Wet oxidation

ABSTRACT

Organic fraction of municipal solid waste is a type of biomass that is attractive due to its marginal cost and suitability for biogas production. The residual product of organic waste digestion is digestate, the high moisture content of which is a problem, even after mechanical dewatering, due to the significant heat requirement for drying. Hydrothermal carbonisation is a process that can potentially offer great benefits by improved mechanical dewatering and valorisation of the digestate into a better-quality solid fuel. However, such valorisation produces liquid by-product effluent rich in organic compounds. Membrane separation could be used to treat such effluent and increase the concentration of the organic compounds while at the same time facilitating the recovery of clean water in the permeate. This work presents the results of the investigation performed using polymeric membranes. The study showed that membrane separation keeps a significant fraction of organics in the retentate. Such concentration significantly increases the biomethane potential of such effluent as well as the energy that could be theoretically used for the generation of process heat using the concentrated retentate in the wet oxidation process.

1. Introduction

Biogas plants are typically associated with lower thermo-ecological costs when compared to other renewable energy sources [1], especially for intermittent energy sources like wind without proper energy storage [2]. Moreover, integrating biogas plants with intermittent renewable energy sources (e.g., photovoltaics) into trigeneration plants could provide effects of synergy such as improved sustainability and lower CO_2 footprint of such installations [3]. Hydrothermal carbonisation (HTC) is promising in terms of the valorisation of various types of wet biomass, including digestates from biogas production [4–7]. HTC is a thermal valorisation process, which takes place in subcritical water at elevated temperatures (typically 170–260 °C) [8–11] with residence time ranging between 30 min and a couple of hours [12–15], and mostly autogenic pressures ranging between 2 and 6 MPa [16] (above saturation pressure for particular temperature). During HTC, complex reaction pathways occur, with different reactions proceeding in parallel [17–19].

* Corresponding author. Wroclaw University of Science and Technology, Faculty of Mechanical and Power Engineering, Department of Energy Conversion Engineering, Wybrzeze Wyspianskiego 27, 50-370 Wroclaw, Poland.
** Corresponding author.
E-mail addresses: agnieszka.urbanowska@pwr.edu.pl (A. Urbanowska), lukasz.niedzwiecki@pwr.edu.pl (L. Niedzwiecki).

https://doi.org/10.1016/j.energy.2023.128524
Received 8 April 2023; Received in revised form 18 July 2023; Accepted 22 July 2023
Available online 24 July 2023

Nomenclature

HTC	hydrothermal carbonisation
HMF	hydroxymethylfurfural
LCA	life cycle assessment
AD	anaerobic digestion
COD	chemical oxygen demand
TOC	total organic cabron
MF	microfiltration
UF	ultrafiltration
NF	nanofiltration
BMP	biomethane potential
DOC	dissolved organic carbon
BOD	biological oxygen demand
CAPEX	capital expenditure
GC-MS	gas chromatograph – mass spectrometer

Hydrolysis decomposes biomass into various monomers and oligomers [18,20], with the rate being diffusion controlled [21]. Products of hydrolysis of cellulose and hemicellulose undergo isomerisation, dehydration, and fermentation, thus creating intermediates [18,20,22]. In the case of proteins, hydrolysis yields amino acids, which subsequently take part in Maillard reactions, forming *N*-containing ring compounds [17]. Soluble lignin, after hydrolysis, forms phenolic compounds [18]. Recalcitrant residues, which have not been significantly decomposed by hydrolysis, form primary hydrochar [18,23]. Hydrolysis is followed by dehydration and decarboxylation [20,22,24]. Dehydration decreases the number of hydroxyl groups (OH) [20]. Intermediates form solid-phase aromatic structures by means of polymerisation, condensation, and aromatisation [18,20,22]. Some intermediates, such as HMF, Diels-Alder reactions, nucleophilic substitution, aldol condensation, acetalisation and ring opening, are also mentioned by the literature [25]. Subsequent precipitation makes secondary hydrochars deposit on the surface of primary hydrochars [18,26].

From the practical perspective, a loss of hydroxyl groups makes hydrochars more hydrophobic, both in terms of decreased equilibrium moisture content [27] and facilitating mechanical dewatering [28–30]. Moreover, the grindability of the hydrochars is also improved as a consequence of the treatment [31,32]. Some studies reported easier pelletising of hydrochars compared to raw biomass [24]. Moreover, a part of inorganic fraction of biomass can be removed during HTC, thus changing ash chemistry for subsequent combustion [33–36]. Furthermore, positive influence of HTC on subsequent pyrolysis has been reported by some studies [37–39]. Some studies have proven hydrochars as effective adsorbents of substances such as isoproturon [40]. Due to these features, HTC of low-quality, high-moisture biomass could lead to effective upcycling of the used feedstock, with optimised energy use, as shown by LCA (Life Cycle Assessment) [41–44].

However, along with some improvements that come with HTC, new problems occur, as the effluent left after mechanical separation of the solid and liquid phase of HTC (also called process water) treated biomass contains significant amounts of a wide variety of organic compounds [45]. Attempts to separate a part of organic fraction in the liquid fraction of HTC products have been performed using membranes [46–48], or distillation [49].

It is possible to utilise the chemical energy contained in the organic fraction by the production of biogas. Xiao et al. [50] proposed HTC pretreatment of algae as a way to break down recalcitrant matter, thus enhancing anaerobic digestion (AD), and confirmed the feasibility of such application by LCA. Marin-Batista et al. [51] reported cumulative yields of CH_4 ranging between 294 and 235 mL/g of volatile solids added for post-HTC process water obtained after HTC of dairy manure performed at 200 °C and 170 °C, respectively. Process water samples from HTC of dairy manure performed at 200 °C and 170 °C contained soluble COD (Chemical Oxygen Demand) as high as 18.3 and 12.8 gO_2/L, respectively [51]. However, process water obtained after HTC of dairy manure at 230 °C yielded lower amounts of biogas, in comparison to untreated dairy manure, despite soluble COD reaching 21.3 gO_2/L [51]. This was attributed to the inhibiting influence of aromatic hydrocarbons, such as 1,3,5-cycloheptatriene, ethyl-benzene, 2-methoxy--phenol, 4-hydroxy-benzenemethanol, produced during HTC at 230 °C [51]. A similar trend was confirmed by another work by Marin-Batista et al. [52], which reported anaerobic digestion of the HTC process water, obtained during HTC of microalgal biomass at 240 °C, performed only slightly better than unprocessed biomass and worse than HTC process water samples obtained at 180 °C and 210 °C. On the other hand, Aragon-Briceño et al. [53] reported the biomethane potential of the process water, after HTC of sewage sludge, reaching 260.0, 277.2, and 225.8 mL of CH_4/g of COD, for process water from HTC at 160, 220, and 250 °C, respectively. Ahmed et al. [29] observed the detrimental influence of HTC residence time on the biomethane potential of the post-HTC effluent from HTC of a mixture of digestate and dewatered sewage sludge at 190 °C, as methane production reached 103, 92 and 84 mL of CH_4/g of COD for the HTC effluents obtained for residence times of 1, 2, and 3 h, respectively.

Wet oxidation is a hydrothermal process during which oxidisable organic and inorganic compounds are degraded at high temperatures in the liquid phase using oxygen [54]. Reported process conditions vary significantly, with reported temperatures ranging between 112 and 350 °C [55,56]. Industrial, non-catalytic wet oxidation processes, such as Zimpro, Wetox, Vertech, Kenox, and Oxyjet, operate within the range of 150 up to 325 °C [55]. Among oxidising agents, one can distinguish oxygen, air, as well as hydrogen peroxide [54–56].

Few works reported results of wet oxidation of post-HTC effluent. Wilk et al. [57] performed wet oxidation at 240 °C, using process water from HTC of sewage sludge performed at 200 °C and 220 °C, with a residence time of 2 h. Wet oxidation at such process conditions allowed reducing COD of HTC effluents from 45.9 (HTC at 200 °C) and 43.5 (HTC at 220 °C) g_{O2}/L to 18.2 and 18.5 g_{O2}/L, respectively [57]. Weiner et al. [58] achieved COD removal of 30–55% by wet oxidation performed at 200 °C, using the effluent from HTC of sewage sludge performed at temperatures between 170 and 210 °C. Wet oxidation performed at 120 °C resulted in a reduction of COD below 10% [58]. Riedel et al. [59] performed wet oxidation at 120–200 °C, using as a feedstock effluent from HTC of brewer's spent grain at 200 °C, achieving COD reduction between 40 and 55%. Toufiq Reza et al. [60] reported decrease of total organic carbon (TOC) reaching 60% for wet air oxidation performed at 260 °C, with effluents from HTC of dairy manure and wastewater sludge digestate performed at 220 °C. Little information is available on requirements for external heat of wet oxidation. On the other hand concentration of organic compounds in retentate, which could be achieved with membrane treatment of HTC effluent with simultaneous decrease of COD in permeate [47,48], could potentially make wet oxidation autothermal. Moreover, the optimisation of cascade membrane systems for the purification of HTC effluents could increase the effect of synergy.

The aim of this work is an optimisation of a cascade system of dead-end polymeric membranes consisting of microfiltration (MF), ultrafiltration (UF), and nanofiltration (NF) used for concentrating organic substances present in the HTC effluent of digestate. Moreover, the aim of this work is to assess possible recovery of energy in the liquid fraction of HTC products. Firstly, the work shows possible increase in biomethane potential (BMP) of retentates, in comparison to liquid fraction of HTC products. Secondly, retentates after membrane filtration of the liquid fraction of HTC products are assessed in terms of the heat that could be obtained through oxidation of the organics present in the liquid effluent, as well as the temperature, which could be achieved during such process.

2. Materials and methods

2.1. HTC of digestate

Samples of the digestate were taken from an agricultural biogas plant owned by Butor Group in Silesia, Poland. A sample of the digestate was taken from a sampling point between AD reactor and mechanical dewatering installation. A diagram of the experimental setup (Fig. 1) shows the autoclave rig. The autoclave was filled with 3.8 L of wet digestate, which had a solid content of 10.1%, determined with Radwag MA. X2.A at 105 °C.

HTC temperature of 190 °C was chosen, based on the literature range between 200 °C and 260 °C [61,62], and taking into account the design preference of industrial scale HTC installations for a lower range of pressure, which allows the comparably lower thickness of reactor's walls and is better from safety perspective [63]. After heating up, the biomass was kept in the reactor for 30 min. Subsequently, the heating was switched off, and the rig was left to cool overnight.

2.2. Cascade membrane filtration

Various types of flat polymeric membranes were used in the tests:

- Microfiltration membrane (MF 0.02 μm) (Hoechst Celgard Corporation), made of 25.4 μm thick polypropylene, 45% porosity, a pore size of 0.02 μm,
- Ultrafiltration membranes (UF) (Microdyn Nadir), made of polyethersulphone (UF PES10, UF PES30) and regenerated cellulose (UF C10 and UF C30) with 10 kDa and 30 kDa MWCO,
- Nanofiltration membranes (NF) (Microdyn Nadir) NPO10P and NPO30P made of polyethersulphone with MWCO in the range 1010–1400 Da and 520–700 Da, as well as Na_2SO_4 retention in the range 25–40% and 80–95%, respectively.

All the tested membranes had an effective filtration surface of 38.5 cm^2. The properties of the test solution (HTC effluent) are shown in Table 1.

The post-HTC liquid was treated in the integrated processes, which was a combination of 3 stages of membrane separation: MF, UF and NF combined in selected variants (Fig. 2) (see Fig. 3).

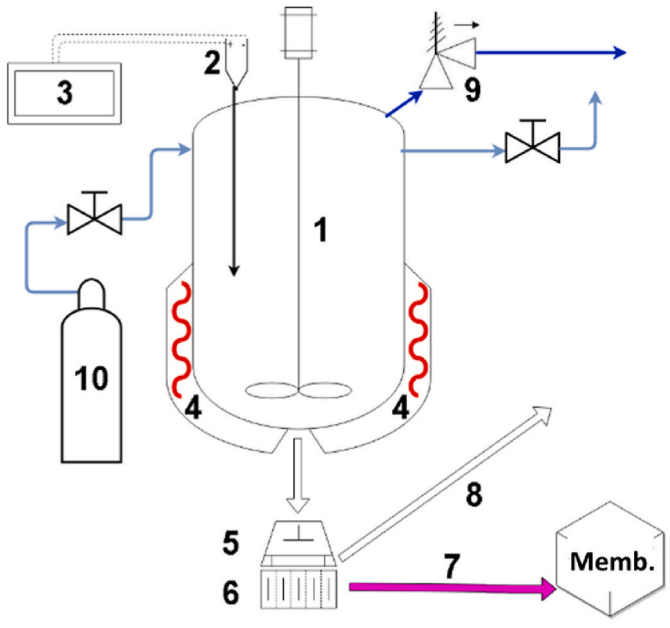

Fig. 1. Diagram of the HTC rig (1 – vessel; 2 –thermocouple; 3 – PLC; 4 – heaters; 5 – cotton filter; 6 – filter's base; 7 – effluent; 8 – separated hydrochar; 9 – safety valve; 10 – purge gas; Memb. – cascade of membranes).

Table 1
Characteristics of the liquid fraction of the HTC digestate from an agricultural biogas plant (COD – chemical oxygen demand; BOD_5 – 5-day biochemical oxygen demand; DOC – dissolved organic carbon).

Index	Value	Unit
pH	7.2	–
Conductivity	14.95	mS/cm
Total suspended solids	3950	mg/L
COD	38,595	mg O_2/L
BOD_5	12,320	mg O_2/L
DOC	23,070	mg C/L
Na	521.3	mg/L
K	1966.5	mg/L
Ca	104.7	mg/L
Mg	101.9	mg/L
Fe	15.9	mg/L
Mn	1.5	mg/L
Cu	0.545	mg/L
Zn	3.977	mg/L
Hg	0.0029	mg/L
Co	0.069	mg/L
Ni	0.147	mg/L

The evaluation of the possibility of sequential purification of the agricultural post-HTC digestate liquid fraction was conducted on a test bench with an Amicon 8400 cell. It is a one-way dead-end flow system with a capacity of 400 mL equipped with a magnetic stirrer to equalise concentrations in the entire volume of solution. The pressure of 0.4 MPa in the system was caused by compressed nitrogen fed from the cylinder.

The process efficiency was determined by measuring the organic compounds concentration expressed as BOD_5, COD and DOC. COD and BOD_5 were determined using standard methods: dichromate and dilution, respectively. The concentration of dissolved organic carbon (DOC) was measured using the HACH IL550 TOC-TN analyser. All treatment experiments were duplicated. Based on the measured factor in raw HTC effluent (c_0) and liquid after membrane filtration (c), removal efficiency (R) for each factor was calculated according to the following equation:

$$R = \frac{c_0 - c}{c_0} \bullet 100, \% \quad (1)$$

The hydraulic capacity of the membranes was determined by determining the permeate flux (J) calculated from equation (2) in which V denotes volume of collected permeate in t time, and A is the membrane surface.

$$J = \frac{V}{A \bullet t}, \frac{mL}{h \bullet cm^2} \quad (2)$$

Vulnerability of membranes to fouling, resulting from deposition on their surface and in the membrane structure of contaminants from the treated solution, and resulting in a decrease in the hydraulic efficiency of the membranes was determined by calculating the relative permeability (J/J_0), where J_0 is the flux measured for distilled water.

2.3. Calculations for determination of biomethane potential and heat effect of retentates in the wet oxidation process

Possibilities of assessing potential for chemical energy recovery from retentates are assessed by looking at the that could be obtained through oxidation of retentates or biomethane potential, i.e., quantities of biomethane present in biogas, which could be produced by anaerobic digestion of the retentates. Chemical energy of biogas can be converted to heat or mechanical energy by combustion of the methane contained in the biogas [64,65].

Equation (3) presents the formula for the calculation of the theoretical biomethane potential (BMP) in the retentate.

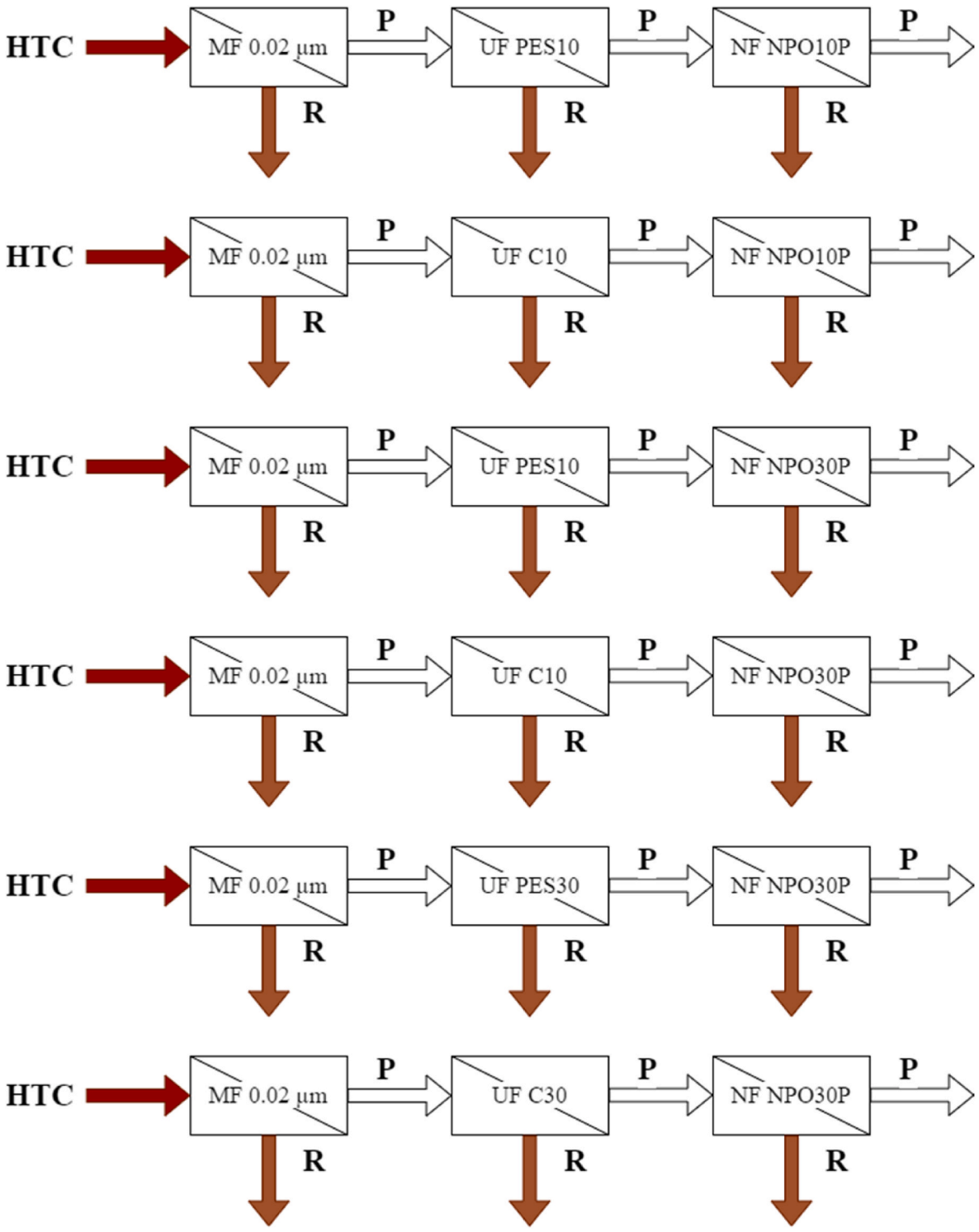

Fig. 2. Different configurations of the cascades membrane systems used in the investigation (R – retentate; P – permeate).

$$BMP_{Th} = 0.39 \bullet COD \bullet \frac{DOC}{COD} \bullet 0.9, L_{CH4}/L_{liquid} \quad (3)$$

To calculate the BMP of the retentate, the stochiometric formula (4) of methane oxidation was used. This formula allows the calculation of the potential amount of methane produced based on the chemical oxygen demand (COD) balance of a sample [66].

The COD conversion to methane at 35 °C is 0.39 L of CH_4 per gram of COD. Furthermore, second correction factors were applied to make the prediction more accurate. The first correction factor referred to the DOC/COD ratio that was used since the COD refers to all the organics and inorganics that can be oxidised and the DOC only to the organic carbon compounds that potentially can be converted into methane. The second correction factor is related to the biodegradability of HTC process water, which is 90%. This factor was based on a comparison of the real BMP reported in previous studies versus the theoretical BMP value from the normal conversion of the stochiometric formula [53,67]:

$$CH_4 + 2O_2 \rightarrow CO_2 + 2H_2O \quad (4)$$

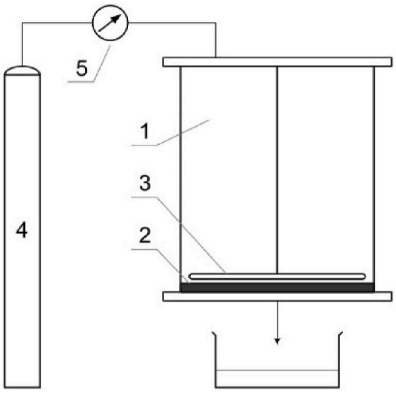

Fig. 3. Amicon 8400 dead-end membrane system (1 - ultrafiltration cell, 2 - membrane, 3 - stirrer, 4 - pressurised nitrogen cylinder, 5 - pressure valve).

The retentates were analysed, in order to identify potential inhibitors of anaerobic digestion, using GC-MS consisting of the Agilent 7820-A GC, with Stabilwax-DA column, and the Agilent 5977 B MSD. NIST-14 MS library was used for compounds' identification using mass spectra with a minimum match factor of 80%.

The heat that could potentially be generated during wet oxidation of the retentate, depending on the filtration time and configuration of membrane cascade, was calculated under the assumption that wet oxidation could reduce the COD of the retentate by 55%, based on values reported by Weiner et al. [58], whereas wet oxidation enthalpy was assumed to be 13.1 ± 0.7 MJ per kg of consumed oxygen, as reported by Riedel et al. [59]. For calculating the achievable temperature during the wet oxidation process, it was assumed that the temperature of retentate before the start wet oxidation process was 20 °C. All performed calculations assumed batch sizes of 1 L, with fluxes measured during the experiments for each of the cascades for nanofiltration as a limiting step for transmembrane pressure of 0.4 MPa (Table 2). Maximum filtration time was assumed to be 1350 min (22.5 h), thus assuming 90 min per day for backflushing of membranes in order to remove the cake layer, thus preventing fouling.

3. Results and discussion

3.1. Results of membrane filtration experiments

The efficiency of sequential purification of the liquid fraction from HTC of an agricultural digestate varies, and the final quality of the solution is determined by the combination of separation properties of the individual membranes. The conducted study showed that the combination of MF, UF and NF resulted in a significant increase in the efficiency of removal of organic compounds from the analysed liquid. This effect was observed for all analysed cases, regardless of the membrane's limiting resolution or its material. The results obtained are shown in Figs. 4 and 5.

Analysis of the efficiency of the self-contained microfiltration process of the HTC effluent showed that the use of a 0.02 μm pore diameter membrane allowed the solution to be purified to a very low degree. The values of DOC, BOD_5 and DOC retention rate in the purified samples of the digestate were, respectively: 14%, 17% and 0.3% (TMP 0.4 MPa). The use of the UF process after MF for further purification of the liquid made it possible to observe an improvement in the efficiency of the separation of organic compounds. It was also found that the final quality of the purified solution is determined by the cut-off (MWCO) of the membrane used. The deterioration in the quality of the purified solution can be easily noticed as the cut-off value, and thus the average pore size increased. This is due to the fact that for a higher cut-off value of the membrane, larger particles of organic pollutants penetrated into the purified solution.

Table 2
Fluxes measured for each of cascade experiments for nanofiltration step.

	J mL/h·cm^2
MF 0.02 μm + UF PES10 + NF NPO10P	0.935
MF 0.02 μm + UF C10 + NF NPO10P	1.870
MF 0.02 μm + UF PES10 + NF NPO30P	0.935
MF 0.02 μm + UF C10 + NF NPO30P	0.904
MF 0.02 μm + UF PES30 + NF NPO30P	0.779
MF 0.02 μm + UF C30 + NF NPO30P	0.686
MF 0.02 μm + UF PES30 + NF NPO10P	0.935
MF 0.02 μm + UF C30 + NF NPO10P	1.403

Analysing the material of the ultrafiltration membrane used in the MF-UF combination, it was found that it had no significant effect on the separation properties of the membranes tested. Both polyethersulfone (PES) and regenerated cellulose (C) caused the content of organic compounds in the permeate to remain at comparable levels. For example, at a constant transmembrane pressure of 0.4 MPa, the R_{DOC}, R_{BOD5} and R_{COD} values, depending on the cut-off of the membrane used, were, respectively: 36–40%, 67–69% and 26–27% (when using a 10 kDa cut-off membrane) and 27–28%, 51–57% and 11–15% (when using a 30 kDa cut-off membrane).

The combination of the three pressure-driven membrane processes analysed allowed a significant improvement in the efficiency of post-HTC digestate purification. This effect was observed in the course of all tested variants of the application of different types of membranes (micro-, ultra- and nanofiltration). The final quality of the permeate was determined by the combination of properties of the successively applied membranes. The values of DOC, BOD_5 and COD retention coefficients obtained for both nanofiltration membranes tested demonstrate how much the composition of the permeate was affected by the type of NF membrane used. It was easy to see that the use of a less dense membrane (NPO10P) resulted in a deterioration of the quality of the final permeate. For example, the NPO30P membrane allowed achieving DOC, BOD_5 and COD retention of 67, 82 and 70%, while the NPO10P membrane allowed reducing DOC, BOD_5 and COD by 57, 74 and 41%, respectively (when preceded by MF 0.02 μm-UF PES 10 sequence). The better separation properties of the NPO30P membrane may result from its dense structure [68]. Membrane filtration results are in good quantitative agreement with other works, e.g., Czerwińska et al. [46] achieved 25.5%, 73.0%, and 84.9% of COD removal efficiency, for ultrafiltration, nanofiltration, and double nanofiltration, respectively.

Based on the results, it was found that the best results, i.e., the best quality of the permeate in terms of organic content, were obtained by conducting sequential treatment in the variant microfiltration (0.02 μm membrane) → ultrafiltration (10 kDa PES membrane) → nanofiltration (NPO30P membrane).

The goal of combining membrane processes, in addition to increasing separation efficiency, is to reduce the intensity of membrane fouling, such as by purifying solutions in integrated systems using sequential membrane processes. The use of the sequence of membrane techniques analysed (Fig. 6) has partially reduced membrane fouling. A comparison of the J/J_0 values obtained in the stand-alone UF and NF processes with those determined for the MF-UF and MF-UF-NF system indicates that the use of prefiltration allows for improving the transport properties of the last membrane in the process chain. MF applied before UF removes some of the compounds blocking the next membrane, while the use of a more compact UF membrane (10 kDa) made of PES or C between MF and NF removes the remaining compounds deposited on the surfaces of NF membranes. The use of a UF membrane with a cut-off of 30 kDa, which has a larger pore size and thus lower contaminant separation efficiency, does not improve the transport properties of NF membranes as significantly since fractions remaining in the permeate can penetrate the pores of NF membranes or settle on their surface, contributing to their blockage. At the same time, it has been observed that the type of

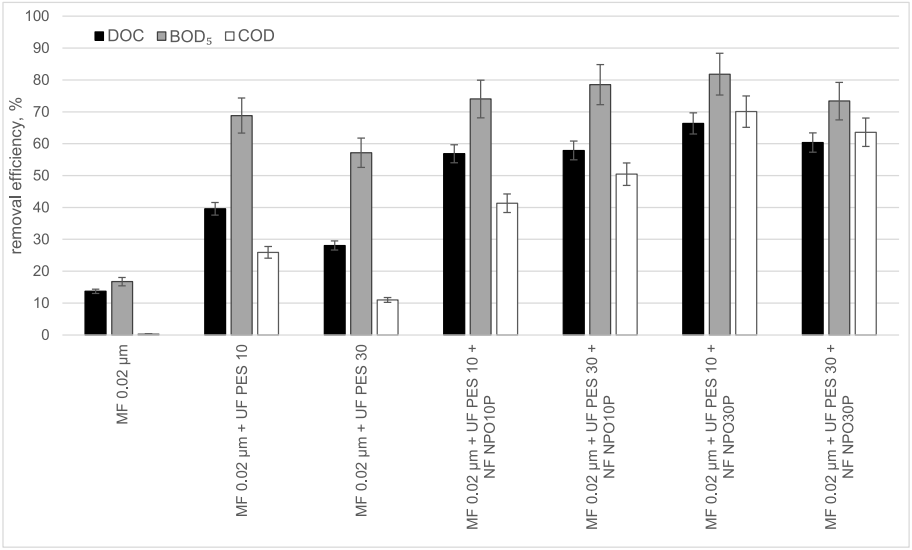

Fig. 4. Efficiency of DOC, BOD_5 and COD removal in different membrane process configurations when using UF membranes made of polyethersulphone.

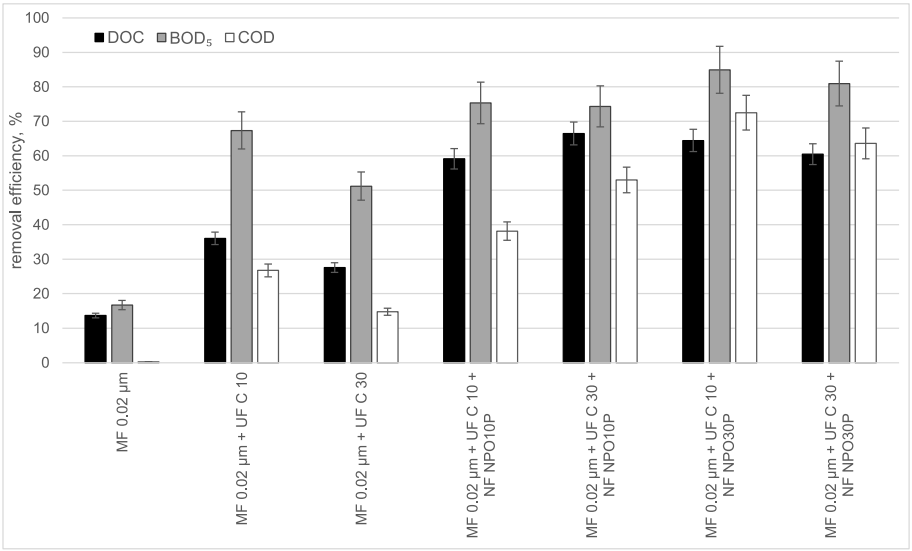

Fig. 5. Efficiency of DOC, BOD_5 and COD removal in different membrane process configurations when using UF membranes made of regenerated cellulose.

membrane used in NF also matters in terms of the membrane's susceptibility to blocking. The values of relative membrane permeability (J/J_0) were when the NPO30P membrane was the final element of the sequence, lower than when the NPO10P membrane was used, which may be due, among other things, to the more compact structure of the second membrane. In this case, its fouling is mainly due to the external blocking phenomenon. According to Kovacs and Samhaber [68], the cut-off value of the NPO10P membrane is higher and is in the range of 1010–1400 Da (with a pore diameter of 0.80–1.29 nm), while that of the NPO30P membrane is in the range of 500–700 Da (with a pore diameter of 0.57–0.93 nm). This may result in higher hydraulic resistance and, thus, lower permeability of NPO30P membranes.

3.2. Biomethane potential of retentates

Based on the achieved densification of chemical energy, expressed as either COD or DOC (Figs. 7 and 8), it could be clearly observed that the separation of organics, using a cascade of dead-end membranes, is a sensible strategy in terms of obtaining the liquid retentate with higher energy generation potential.

Fig. 9 clearly shows that significant densification of chemical energy could be achieved, increasing the biomethane potential from approx. 5 L of methane for liquid effluent from HTC up to almost 200 L of methane for retentates' mixture from all levels of the cascade after a whole day of dead-end membrane separation. It should be noted that it will not increase the total energy that could be recovered since the volume of the retentate will be much smaller than the volume of post-HTC effluent. However, as a consequence of chemical energy densification, the biogas reactor could be much smaller in comparison to the reactor for the untreated effluent, cutting down on the CAPEX of such installation. Moreover, much less inoculum would be needed in order to maintain the desired solid ratio in such a reactor. Furthermore, if the production of biogas from the retentates got integrated with the primary anaerobic digestion reactor (source of the digestate), recalculation of the retentates would not have such an extensive influence on the solid ratio in the reactor, in comparison to recirculation of untreated post-HTC effluent. Results obtained for the cascades consisting of MF 0.02 µm + UF C10 + NF NPO10P as well as MF 0.02 µm + UF C30 + NF NPO10P it can be clearly seen that even higher relative ratios of batch size to the membrane surface of dead-end membranes could be achieved, thus enabling

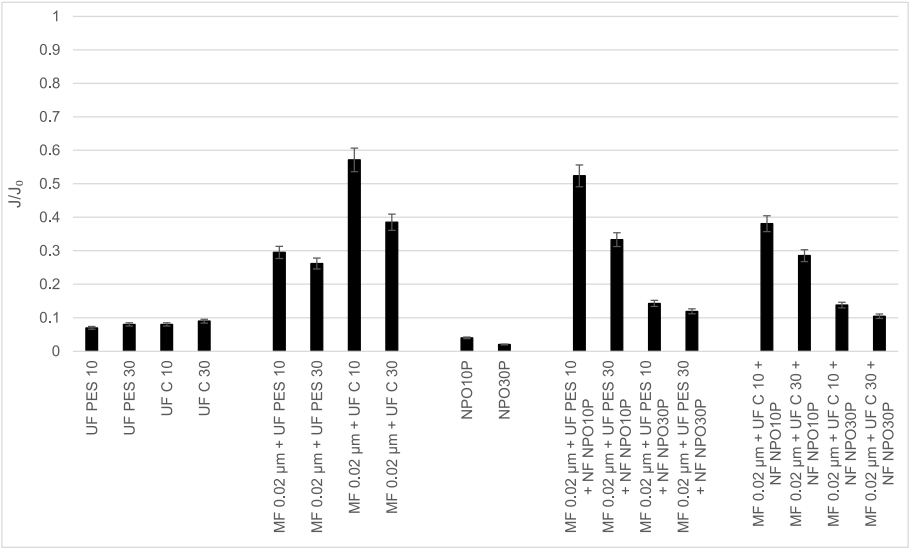

Fig. 6. Relative membrane permeability in different membrane process configurations (in the case of a sequence of processes, the J/J_0 of the last process is given).

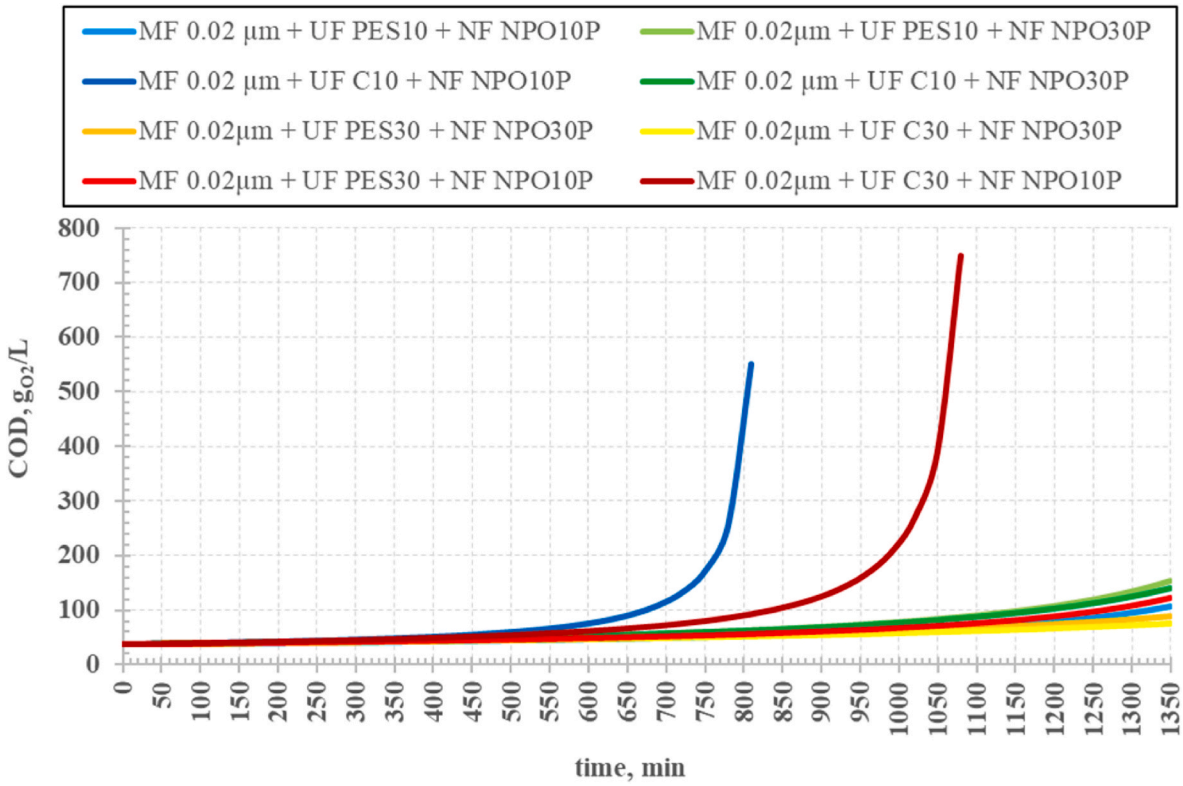

Fig. 7. Increase of COD with increased filtration time for different configuration of membrane cascades.

processing of bigger batches for the same membrane surface area, during 24 h operation. Thus, relatively lower investment costs could be achieved for these cascades.

Some researchers approached recovery of chemical energy from retentates after membrane filtration of wastewater in similar manner, i.e., by using the organics in retentate to produce biogas. Luo et al. [69] suggested the use of retentate from membrane filtration of diary wastewater, containing high concentration of organics, as a substrate for production of biogas. Chen et al. [70] suggested an integrated process, consisting of isoelectric precipitation, nanofiltration and anaerobic digestion as a way of utilisation of organics in the dairy wastewater. The study reported increased production of acetate, butyrate, and hydrogen, using a nanofiltration retentate as substrate. Campell et al. [71] mixed performed anaerobic digestion of HTC process water before and after nanofiltration and reverse osmosis treatment. The retentates achieved 93.5% COD degradation during anaerobic digestion, comparing to 69.6% COD degradation of untreated HTC process water. Aragón-Briceño et al. [53] reported increased COD degradation efficiency for process waters after HTC of sewage sludge, in comparison to sewage sludge digestate. Digestate achieved COD degradation of 56.6%, in comparison to 69.1%, 79.6%, and 63.8%, for process waters from HTC of sewage sludge performed at 160 °C, 220 °C, and 250 °C, respectively.

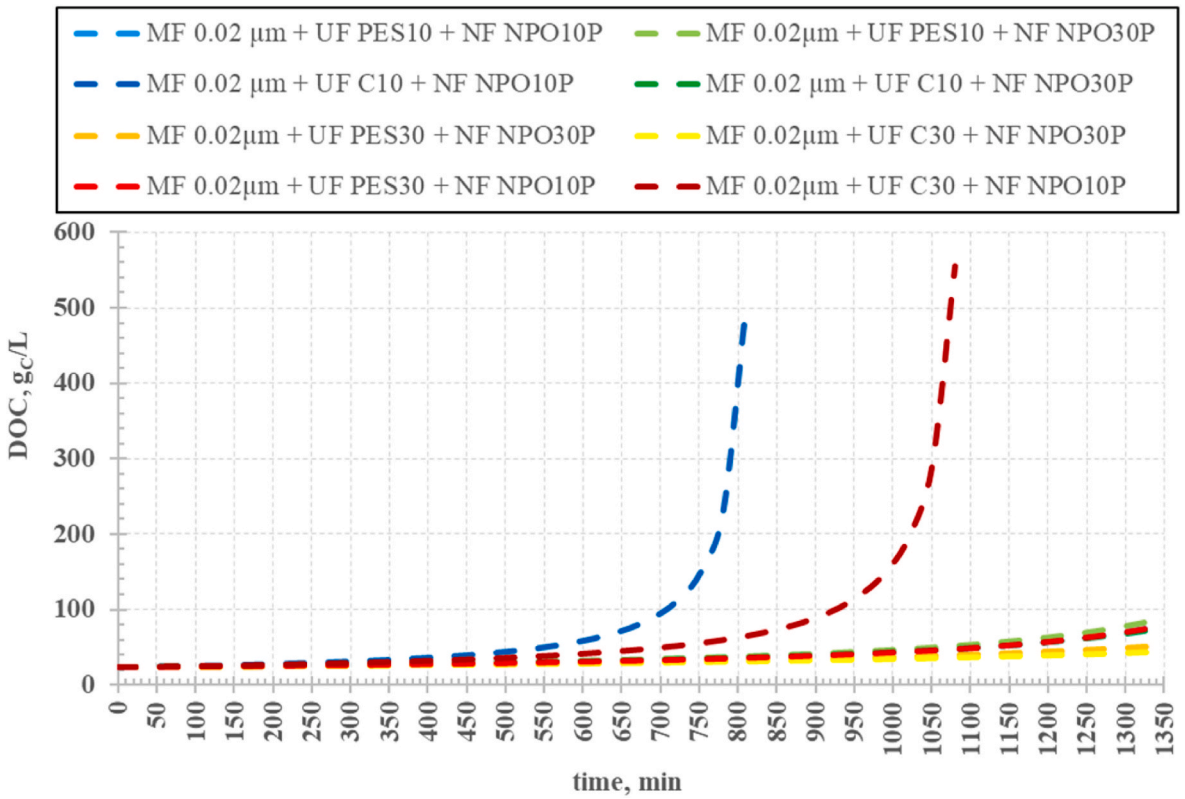

Fig. 8. Increase of DOC with increased filtration time for different configuration of membrane cascades.

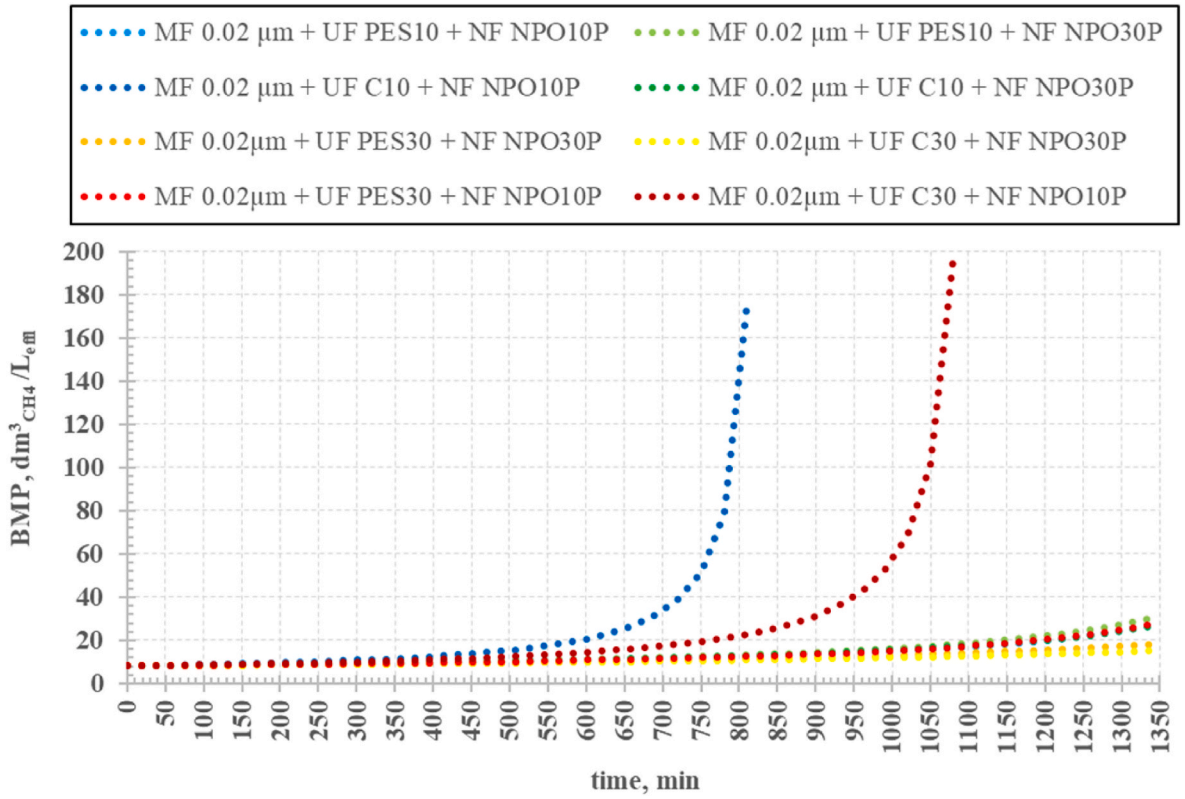

Fig. 9. Increasing BMP of the retentate depending on the filtration time and configuration of membrane cascade.

Parmar and Ross [72] obtained methane yields ranging between 100 and 180 mL_{CH4}/g_{COD} for anaerobic digestion of HTC process water from HTC of sewage sludge and agricultural residues. De la Rubia et al. [73] reported methane yields ranging between 99 and 177 mL_{CH4}/g_{COD} for anaerobic digestion of HTC process water from HTC of dewatered sewage sludge at 208 °C, depending on the source of inoculum. This suggests that resilience of microbial culture is an important factor. Therefore, it is important to look for possible inhibitors of anaerobic digestion process in the liquid fraction of HTC products, especially retentates after filtration, for which concentrations might increase, in comparison to the process water.

GC-MS analysis (Table 3) has shown that the compounds present in the retentates consisted of heterocyclic compounds (mainly pyrazine and its isomers), volatile fatty acids (acetic acid, propanoic acid, butanoic acid), as well as other carboxylic acids containing phenyl group (hydrocinnamic acid, benzeneacetic acid), phenol, and 3-Pyridinol. No clear trend could be observed regarding the retention of these compounds by the membrane cascades, which could be attributed to the fact that the cut-off of NF membranes [47] was an order of magnitude bigger than the atomic masses of detected compounds. This suggests that any retention of volatile organic compounds in the retentate could be attributed to interaction with filtering cake on the surfaces of the membranes rather than to membrane separation properties.

Among the detected compounds, those with significantly high peaks were quantified (Table 3). Volatile fatty acids are products of acidogenesis [74,75], and others are still present among products of acetogenesis [74], which are used by methanogenic bacterial communities. Some of the pyrazines used to be applied as flavouring agents [76]. Some bacteria produce pyrazines [77]. However, in some cases, excess metabolites are known to exhibit a detrimental influence on microbial communities' growth. Moreover, Marin-Batista et al. [51] reported that pyrazines could be consumed during the anaerobic digestion process. However, De la Rubia et al. [73] reported that consumption of pyrazine, 2,5-dimethyl from HTC process water varied substantially, depending on inoculum, with removal rates for the compound being 0%, 23%, and 88%, for granular inoculum obtained from an internal circulation anaerobic reactor treating brewery wastewater, granular anaerobic sludge from an up-flow anaerobic sludge blanket reactor treating sugar beet effluent, and flocculent anaerobic sludge from a sewage sludge digester, respectively. Moreover, 2,5-bis(1-methylethyl)-pyrazine antimicrobial influence has been proven [78]. However, concentrations of dominating pyrazine isomers detected in retentates (Table 3) were relatively low. Regarding compounds detected with qualitative GC-MS analysis, the antimicrobial influence of 3-pirydinol is not known. However, it has been used, along with Co(II) 3,5-difluorobenzoate, to synthesise antibiotics [79]. Phenols are known for their detrimental influence on biogas production [80]. However, such influence is known for concentrations >2 g/L [80], which is not the case for retentates' solutions within the scope of this study. Overall, inhibitive influence of detected organic compounds seems to be unlikely. However, further experimental research on biomethane potential of highly concentrated retentates is needed to confirm this hypothesis. It might be that other measures, e.g., pH adjustment, would be needed to maintain stable biogas production with highly concentrated retentates.

3.3. Wet oxidation of retentates

Such densification of chemical energy has even more significant consequences when wet oxidation is used to convert such chemical energy into process heat. In terms of the potential, the shape of the curve for wet oxidation (Fig. 10) looks similar to the BMP curve (Fig. 9). However, the practical consequences for the process are much more profound since significant densification allows for achieving higher temperatures of the effluent in the wet oxidation process (Fig. 11).

For optimised membrane cascades, retentates during wet oxidation could achieve temperatures within the supercritical region exceeding 580 °C, which is much higher than the HTC temperature. However, this is also the temperature much higher than the critical point for water (373.946 °C, 22.064 MPa), which would make oxidation perform in the supercritical region. Such hot liquid, after wet oxidation, would greatly facilitate optimisation of process heat supply to HTC reactor, thus allowing effective recovery of chemical energy, which would otherwise be wasted. However, such high temperatures are not needed either for wet oxidation or for HTC. What can be seen in Fig. 11 is that a couple of different cascades of membranes are capable of sufficiently concentrating a batch of effluent to make it exceed 200 °C and, at the same time, provide a possibility to operate wet oxidation as an autothermal process, without supplying an external source of heat.

4. Conclusions

The research presented in this paper has shown that a significant densification of chemical energy in the retentates could be achieved using a cascade membrane system. An increase in the BMP for densified retentates' mixture facilitates optimisation of the solid ratio of biogas reactors as well as the CAPEX of such investment in energy recovery from the liquid HTC by-products through anaerobic digestion. An increase of the maximum temperature, which could be achieved during the wet oxidation process due to chemical energy densification, is significant for the optimised conversion of chemical energy in the liquid post-HTC effluent when converting to process heat for HTC. Temperatures exceeding the temperature of the HTC process could be easily achieved, thus allowing for effective heat recovery, with ΔT sufficient for heat exchangers reasonable in size. The screening mechanisms combination of sequentially connected membranes significantly increases the organic compounds removing effectiveness from the agricultural digestate liquid fraction. Overall, biomethane potential as high as 200 $L_{CH4}/L_{retentate}$ could be expected. Moreover, for most cascades, it is possible to concentrate the chemical energy in the retentate high enough to make wet oxidation autothermal. Further research is required

Table 3
Quantitative GC-MS analysis for selected compounds (c – concentration; U – uncertainty).

	Pyrazine		Pyrazine, 2,5-dimethyl		Pyrazine, ethyl-		Acetic acid		Acetamide		Hydrocinnamic acid	
	mg/L		mg/L		mg/L		mg/L		mg/L		mg/L	
	c	U	c	U	c	U	c	U	c	U	c	U
MF 0.02 μm	31.51	±8.14	25.38	±9.17	25.63	±9.10	87.62	±238.02	16.55	±16.81	79.24	±39.28
MF 0.02 μm + UF PES10	31.88	±7.16	28.85	±8.30	27.81	±8.32	397.28	±237.84	41.26	±16.60	58.89	±32.07
MF 0.02 μm + UF PES10 + NF NPO10P	39.54	±9.93	30.27	±10.55	29.31	±10.50	62.11	±237.83	16.35	±16.65	55.98	±31.86
MF 0.02 μm + UF C10 + NF NPO10P	37.93	±7.65	29.84	±8.58	28.66	±8.55	237.61	±237.96	10.70	±16.60	63.61	±31.83
MF 0.02 μm + UF PES10 + NF NPO30P	25.46	±7.13	16.55	±8.30	12.06	±8.31	60.14	±237.83	11.93	±16.60	56.55	±31.80
MF 0.02 μm + UF C10 + NF NPO30P	24.77	±7.11	16.28	±8.30	11.85	±8.30	58.32	±237.80	12.04	±16.60	55.71	±31.80
MF 0.02 μm + UF PES30	35.19	±7.10	28.65	±8.31	27.32	±8.31	132.72	±237.92	50.52	±16.60	59.28	±31.81
MF 0.02 μm + UF PES30 + NF NPO30P	26.87	±7.10	16.41	±8.31	12.32	±8.30	58.59	±238.01	11.76	±16.60	56.94	±31.81
MF 0.02 μm + UF C30	34.02	±7.10	27.91	±8.32	27.64	±8.30	84.17	±237.83	41.44	±16.60	60.26	±31.81
MF 0.02 μm + UF C30 + NF NPO30P	25.75	±7.11	15.81	±8.30	11.95	±8.30	56.99	±237.80	52.21	±16.60	57.17	±31.80

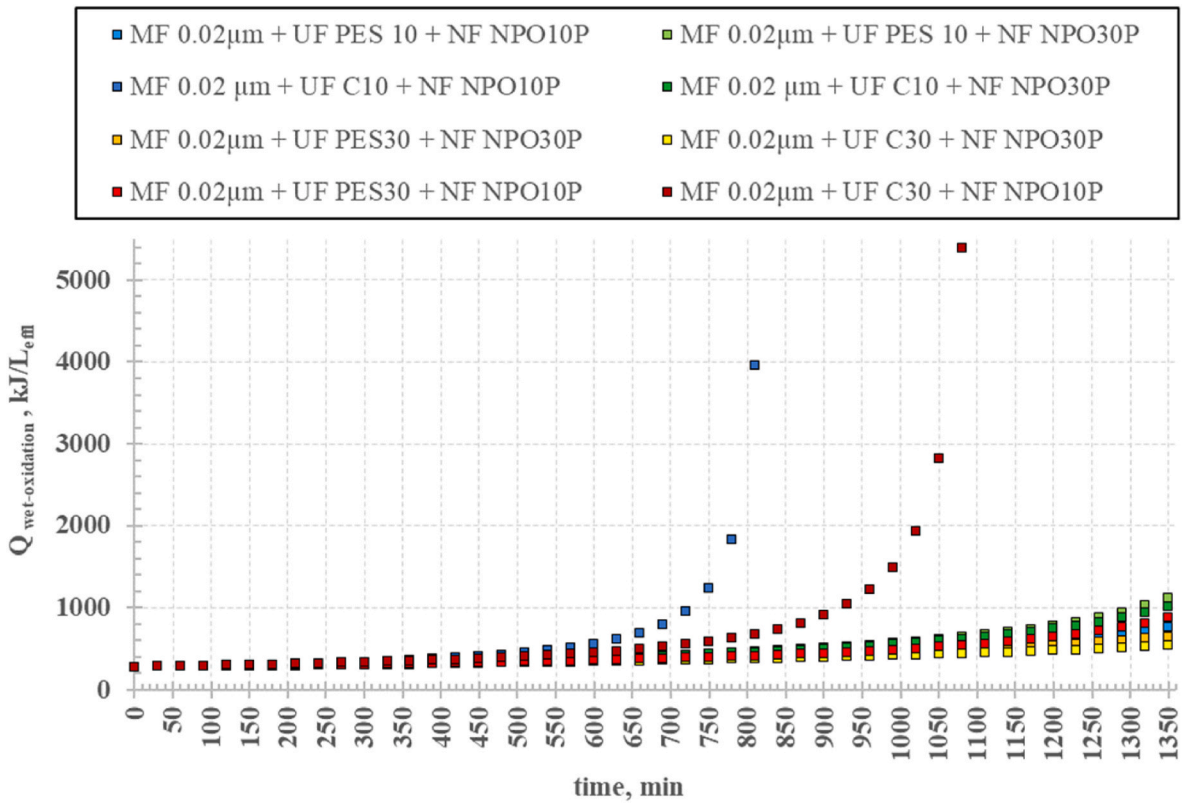

Fig. 10. Increasing the heat potential for wet oxidation of the retentate, depending on the filtration time and configuration of membrane cascade.

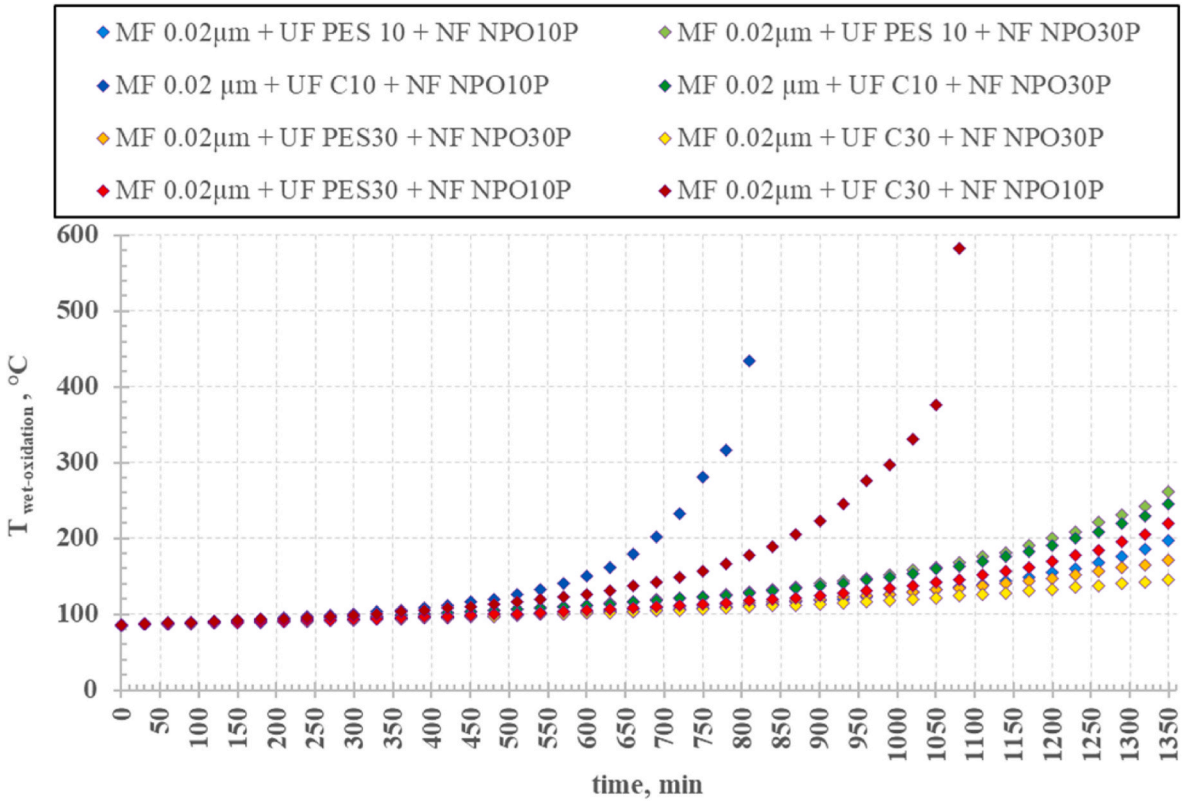

Fig. 11. Increasing the achievable wet oxidation temperature for the retentate, depending on the filtration time and configuration of membrane cascade.

to obtain empirical verification of the results of the performed assessment.

Credit author statement

Agnieszka Urbanowska: Conceptualization, Methodology, Validation, Formal analysis, Investigation, Writing—original draft preparation, Writing—review and editing, Funding acquisition. Lukasz Niedzwiecki: Conceptualization, Methodology, Formal analysis, Writing—original draft preparation, Writing—review and editing. Mateusz Wnukowski: Methodology, Validation, Formal analysis, Investigation. Christian Aragon-Briceño: Methodology, Validation, Formal analysis, Writing—original draft preparation, Writing—review and editing. Małgorzata Kabsch-Korbutowicz: Methodology, Validation, Writing—review and editing, Supervision. Marcin Baranowski: Investigation, Data curation. Michał Czerep: Investigation, Data curation. Przemysław Seruga: Data curation, Project administration, Funding acquisition. Halina Pawlak-Kruczek: Resources, Project administration, Funding acquisition, Supervision. Eddy Bramer: Resources, Funding acquisition, Supervision. Gerrit Brem: Resources, Funding acquisition, Supervision. Artur Pożarlik: Resources, Project administration, Funding acquisition, Supervision, Writing—review and editing.

Declaration of competing interest

The authors declare that they have no known competing financial interests or personal relationships that could have appeared to influence the work reported in this paper.

Data availability

Data will be made available on request.

Acknowledgements

The Authors would like to thank the European Commission, the National Center for Research and Development (Poland), Nederlandse Organisatie Voor Wetenschappelijk Onderzoek (Netherlands) and Swedish Research Council Formas for funding in the frame of the collaborative international consortium (RECOWATDIG) financed under the 2018 Joint call of the WaterWorks2017 ERA-NET Cofund. This ERA-NET is an integral part of the activities developed by the Water JPI. National Centre for Research and Development agreement number WATERWORKS2017/I/RECOWATDIG/01/2019. Authors would like to thank Butor Group for providing digestate for the research.

References

[1] Stanek W, Czarnowska L, Gazda W, Simla T. Thermo-ecological cost of electricity from renewable energy sources. Renew Energy 2018;115:87–96. https://doi.org/10.1016/j.renene.2017.07.074.
[2] Simla T, Stanek W. Reducing the impact of wind farms on the electric power system by the use of energy storage. Renew Energy 2020;145:772–82. https://doi.org/10.1016/j.renene.2019.06.028.
[3] Gazda W, Stanek W. Energy and environmental assessment of integrated biogas trigeneration and photovoltaic plant as more sustainable industrial system. Appl Energy 2016;169:138–49. https://doi.org/10.1016/j.apenergy.2016.02.037.
[4] Aragón-Briceño CI, Ross AB, Camargo-Valero MA. Mass and energy integration study of hydrothermal carbonization with anaerobic digestion of sewage sludge. Renew Energy 2021;167:473–83. https://doi.org/10.1016/j.renene.2020.11.103.
[5] Aragon-Briceño C, Pożarlik A, Bramer E, Brem G, Wang S, Wen Y, et al. Integration of hydrothermal carbonization treatment for water and energy recovery from organic fraction of municipal solid waste digestate. Renew Energy 2022;184:577–91. https://doi.org/10.1016/j.renene.2021.11.106.
[6] Numviyimana C, Warchoł J, Khalaf N, Leahy JJ, Chojnacka K. Phosphorus recovery as struvite from hydrothermal carbonization liquor of chemically produced dairy sludge by extraction and precipitation. J Environ Chem Eng 2022;10. https://doi.org/10.1016/j.jece.2021.106947.
[7] Mlonka-Mędrala A, Sieradzka M, Magdziarz A. Thermal upgrading of hydrochar from anaerobic digestion of municipal solid waste organic fraction. Fuel 2022;324:124435. https://doi.org/10.1016/j.fuel.2022.124435.
[8] Śliz M, Wilk M. A comprehensive investigation of hydrothermal carbonization: energy potential of hydrochar derived from Virginia mallow. Renew Energy 2020;156:942–50. https://doi.org/10.1016/j.renene.2020.04.124.
[9] Wilk M, Magdziarz A, Kalemba-Rec I, Szymańska-Chargot M. Upgrading of green waste into carbon-rich solid biofuel by hydrothermal carbonization: the effect of process parameters on hydrochar derived from acacia. Energy 2020;202:117717. https://doi.org/10.1016/j.energy.2020.117717.
[10] Magdziarz A, Wilk M, Wądrzyk M. Pyrolysis of hydrochar derived from biomass – experimental investigation. Fuel 2020;267. https://doi.org/10.1016/j.fuel.2020.117246.
[11] Magdziarz A, Mlonka-Mędrala A, Sieradzka M, Aragon-Briceño C, Pożarlik A, Bramer EA, et al. Multiphase analysis of hydrochars obtained by anaerobic digestion of municipal solid waste organic fraction. Renew Energy 2021;175:108–18. https://doi.org/10.1016/j.renene.2021.05.018.
[12] Kumar N, Weldon R, Lynam JG. Hydrothermal carbonization of coffee silverskins. Biocatal Agric Biotechnol 2021;36:102145. https://doi.org/10.1016/j.bcab.2021.102145.
[13] Sobek S, Tran Q-K, Junga R, Werle S. Hydrothermal carbonization of the waste straw: a study of the biomass transient heating behavior and solid products combustion kinetics. Fuel 2022;314:122725. https://doi.org/10.1016/j.fuel.2021.122725.
[14] Smith AM, Ekpo U, Ross AB. The influence of pH on the combustion properties of bio-coal following hydrothermal treatment of swine manure. Energies 2020;13:1–20. https://doi.org/10.3390/en13020331.
[15] Azaare L, Commeh MK, Smith AM, Kemausuor F. Co-hydrothermal carbonization of pineapple and watermelon peels: effects of process parameters on hydrochar yield and energy content. Bioresour Technol Rep 2021;15:100720. https://doi.org/10.1016/j.biteb.2021.100720.
[16] Mumtaz H, Sobek S, Werle S, Sajdak M, Muzyka R. Hydrothermal treatment of plastic waste within a circular economy perspective. Sustain Chem Pharm 2023;32:100991. https://doi.org/10.1016/j.scp.2023.100991.
[17] Djandja OS, Yin L-X, Wang Z-C, Duan P-G. From wastewater treatment to resources recovery through hydrothermal treatments of municipal sewage sludge: a critical review. Process Saf Environ Protect 2021;151:101–27. https://doi.org/10.1016/j.psep.2021.05.006.
[18] Picone A, Volpe M, Messineo A. Process water recirculation during hydrothermal carbonization of waste biomass: current knowledge and challenges. Energies 2021;14:2962. https://doi.org/10.3390/en14102962.
[19] Kossińska N, Krzyżyńska R, Ghazal H, Jouhara H. Hydrothermal carbonisation of sewage sludge and resulting biofuels as a sustainable energy source. Energy 2023:127337. https://doi.org/10.1016/j.energy.2023.127337.
[20] Funke A, Ziegler F. Hydrothermal carbonisation of biomass: a summary and discussion of chemical mechanisms for process engineering. Biofuels, Bioprod Biorefining 2010;4:160–77. https://doi.org/10.1002/bbb.198.
[21] Reza MT, Yan W, Uddin MH, Lynam JG, Hoekman SK, Coronella CJ, et al. Reaction kinetics of hydrothermal carbonization of loblolly pine. Bioresour Technol 2013;139:161–9. https://doi.org/10.1016/j.biortech.2013.04.028.
[22] Reza MT, Andert J, Wirth B, Busch D, Pielert J, Lynam JG, et al. Hydrothermal carbonization of biomass for energy and crop production. Appl Bioenergy 2014;1:11–29. https://doi.org/10.2478/apbi-2014-0001.
[23] Pawlak-Kruczek H, Niedzwiecki L, Sieradzka M, Mlonka-Mędrala A, Baranowski M, Serafin-Tkaczuk M, et al. Hydrothermal carbonization of agricultural and municipal solid waste digestates – structure and energetic properties of the solid products. Fuel 2020;275:117837. https://doi.org/10.1016/j.fuel.2020.117837.
[24] Funke A, Ziegler F. Heat of reaction measurements for hydrothermal carbonization of biomass. Bioresour Technol 2011;102:7595–8. https://doi.org/10.1016/j.biortech.2011.05.016.
[25] Baccile N, Falco C, Titirici MM. Characterization of biomass and its derived char using 13C-solid state nuclear magnetic resonance. Green Chem 2014;16:4839–69. https://doi.org/10.1039/c3gc42570c.
[26] Lucian M, Volpe M, Gao L, Piro G, Goldfarb JL, Fiori L. Impact of hydrothermal carbonization conditions on the formation of hydrochars and secondary chars from the organic fraction of municipal solid waste. Fuel 2018;233:257–68. https://doi.org/10.1016/j.fuel.2018.06.060.
[27] Acharjee TC, Coronella CJ, Vasquez VR. Effect of thermal pretreatment on equilibrium moisture content of lignocellulosic biomass. Bioresour Technol 2011;102:4849–54. https://doi.org/10.1016/j.biortech.2011.01.018.
[28] Gao N, Li Z, Quan C, Miskolczi N, Egedy A. A new method combining hydrothermal carbonization and mechanical compression in-situ for sewage sludge dewatering: bench-scale verification. J Anal Appl Pyrolysis 2019;139:187–95. https://doi.org/10.1016/j.jaap.2019.02.003.
[29] Ahmed M, Andreottola G, Elagroudy S, Negm MS, Fiori L. Coupling hydrothermal carbonization and anaerobic digestion for sewage digestate management: influence of hydrothermal treatment time on dewaterability and bio-methane production. J Environ Manag 2021;281:111910. https://doi.org/10.1016/j.jenvman.2020.111910.
[30] Wang L, Zhang L, Li A. Hydrothermal treatment coupled with mechanical expression at increased temperature for excess sludge dewatering: influence of operating conditions and the process energetics. Water Res 2014;65:85–97. https://doi.org/10.1016/j.watres.2014.07.020.
[31] Sharma HB, Panigrahi S, Dubey BK. Hydrothermal carbonization of yard waste for solid bio-fuel production: study on combustion kinetic, energy properties, grindability and flowability of hydrochar. Waste Manag 2019;91:108–19. https://doi.org/10.1016/j.wasman.2019.04.056.
[32] Kambo HS, Dutta A. Comparative evaluation of torrefaction and hydrothermal carbonization of lignocellulosic biomass for the production of solid biofuel. Energy

Convers Manag 2015;105:746–55. https://doi.org/10.1016/j.enconman.2015.08.031.
[33] Smith AM, Singh S, Ross AB. Fate of inorganic material during hydrothermal carbonisation of biomass: influence of feedstock on combustion behaviour of hydrochar. Fuel 2016;169:135–45. https://doi.org/10.1016/j.fuel.2015.12.006.
[34] Smith AM, Whittaker C, Shield I, Ross AB. The potential for production of high quality bio-coal from early harvested Miscanthus by hydrothermal carbonisation. Fuel 2018;220:546–57. https://doi.org/10.1016/j.fuel.2018.01.143.
[35] Smith AM, Ross AB. The influence of residence time during hydrothermal carbonisation of miscanthus on bio-coal combustion chemistry. Energies 2019;12:523. https://doi.org/10.3390/en12030523.
[36] Smith AM, Ross AB. Production of bio-coal, bio-methane and fertilizer from seaweed via hydrothermal carbonisation. Algal Res 2016;16:1–11. https://doi.org/10.1016/j.algal.2016.02.026.
[37] Duan Y, Ning Y, Gao N, Quan C, Grammelis P, Boutikos P. Effect of hydrothermal process on the pyrolysis of oily sludge: characterization and analysis of pyrolysis products. Fuel 2023;338:127347. https://doi.org/10.1016/j.fuel.2022.127347.
[38] Wen Y, Wang S, Shi Z, Nuran Zaini I, Niedzwiecki L, Aragon-Briceno C, et al. H2-rich syngas production from pyrolysis of agricultural waste digestate coupled with the hydrothermal carbonization process. Energy Convers Manag 2022;269:116101. https://doi.org/10.1016/j.enconman.2022.116101.
[39] Wang S, Wen Y, Shi Z, Niedzwiecki L, Baranowski M, Czerep M, et al. Effect of hydrothermal carbonization pretreatment on the pyrolysis behavior of the digestate of agricultural waste: a view on kinetics and thermodynamics. Chem Eng J 2022;431:133881. https://doi.org/10.1016/j.cej.2021.133881.
[40] Mokrzycki J, Lorenc-Grabowska E, Kordek-Khalil K, Rutkowski P. Hydrothermal and pyrolytic biochars from waste milk thistle (Silybum marianum) extrudates as precursors for production of effective isoproturon adsorbents. J Water Process Eng 2020;37:101459. https://doi.org/10.1016/j.jwpe.2020.101459.
[41] Mayer F, Bhandari R, Gäth SA. Life cycle assessment on the treatment of organic waste streams by anaerobic digestion, hydrothermal carbonization and incineration. Waste Manag 2021;130:93–106. https://doi.org/10.1016/j.wasman.2021.05.019.
[42] Stobernack N, Mayer F, Malek C, Bhandari R. Evaluation of the energetic and environmental potential of the hydrothermal carbonization of biowaste: modeling of the entire process chain. Bioresour Technol 2020;318:124038. https://doi.org/10.1016/j.biortech.2020.124038.
[43] Medina-Martos E, Istrate IR, Villamil JA, Gálvez-Martos JL, Dufour J, Mohedano ÁF. Techno-economic and life cycle assessment of an integrated hydrothermal carbonization system for sewage sludge. J Clean Prod 2020;277. https://doi.org/10.1016/j.jclepro.2020.122930.
[44] Mendecka B, Lombardi L, Micali F, Risi A De. Energy recovery from olive pomace by hydrothermal carbonization on hypothetical industrial scale : a LCA perspective. Waste Biomass Valorization 2020. https://doi.org/10.1007/s12649-020-01212-0.
[45] Jackowski M, Semba D, Trusek A, Wnukowski M, Niedzwiecki L, Baranowski M, et al. Hydrothermal carbonization of brewery's spent grains for the production of solid biofuels. Beverages 2019;5:12. https://doi.org/10.3390/beverages5010012.
[46] Czerwińska K, Marszałek A, Kudlek E, Śliz M, Dudziak M, Wilk M. The treatment of post-processing liquid from the hydrothermal carbonization of sewage sludge. Sci Total Environ 2023;885:163858. https://doi.org/10.1016/j.scitotenv.2023.163858.
[47] Urbanowska A, Kabsch-Korbutowicz M, Aragon-Briceño C, Wnukowski M, Pożarlik A, Niedzwiecki L, et al. Cascade membrane system for separation of water and organics from liquid by-products of HTC of the agricultural digestate—evaluation of performance. Energies 2021;14:4752. https://doi.org/10.3390/en14164752.
[48] Urbanowska A, Kabsch-Korbutowicz M, Wnukowski M, Seruga P, Baranowski M, Pawlak-Kruczek H, et al. Treatment of liquid by-products of hydrothermal carbonization (HTC) of agricultural digestate using membrane separation. Energies 2020;13:1–12. https://doi.org/10.3390/en13010262.
[49] Czerwińska K, Śliz M, Wilk M. Thermal disposal of post-processing water derived from the hydrothermal carbonization process of sewage sludge. Waste and Biomass Valorization 2023. https://doi.org/10.1007/s12649-023-02162-z.
[50] Xiao C, Fu Q, Liao Q, Huang Y, Xia A, Chen H, et al. Life cycle and economic assessments of biogas production from microalgae biomass with hydrothermal pretreatment via anaerobic digestion. Renew Energy 2020;151:70–8. https://doi.org/10.1016/j.renene.2019.10.145.
[51] Marin-Batista JD, Villamil JA, Qaramaleki SV, Coronella CJ, Mohedano AF, Rubia MA d. la. Energy valorization of cow manure by hydrothermal carbonization and anaerobic digestion. Renew Energy 2020;160:623–32. https://doi.org/10.1016/j.renene.2020.07.003.
[52] Marin-Batista JD, Villamil JA, Rodriguez JJ, Mohedano AF, de la Rubia MA. Valorization of microalgal biomass by hydrothermal carbonization and anaerobic digestion. Bioresour Technol 2019;274:395–402. https://doi.org/10.1016/j.biortech.2018.11.103.
[53] Aragón-Briceño C, Ross ABB, Camargo-Valero MAA. Evaluation and comparison of product yields and bio-methane potential in sewage digestate following hydrothermal treatment. Appl Energy 2017;208:1357–69. https://doi.org/10.1016/j.apenergy.2017.09.019.
[54] Menoni L, Bertanza G. Wet Oxidation of sewage sludge: a mathematical model for estimating the performance based on the VSS/TSS ratio. Chem Eng J 2016;306:685–92. https://doi.org/10.1016/j.cej.2016.07.105.
[55] Bhargava SK, Tardio J, Prasad J, Föger K, Akolekar DB, Grocott SC. Wet oxidation and catalytic wet oxidation. Ind Eng Chem Res 2006;45:1221–58. https://doi.org/10.1021/ie051059n.
[56] Baroutian S, Smit AM, Andrews J, Young B, Gapes D. Hydrothermal degradation of organic matter in municipal sludge using non-catalytic wet oxidation. Chem Eng J 2015;260:846–54. https://doi.org/10.1016/j.cej.2014.09.063.
[57] Wilk M, Czerwińska K, Śliz M, Imbierowicz M. Hydrothermal carbonization of sewage sludge: hydrochar properties and processing water treatment by distillation and wet oxidation. Energy Rep 2023;9:39–58. https://doi.org/10.1016/j.egyr.2023.03.092.
[58] Weiner B, Breulmann M, Wedwitschka H, Fühner C, Kopinke F-D. Wet oxidation of process waters from the hydrothermal carbonization of sewage sludge. Chem Ing Tech 2018;90:872–80. https://doi.org/10.1002/cite.201700050.
[59] Riedel G, Koehler R, Poerschmann J, Kopinke FD, Weiner B. Combination of hydrothermal carbonization and wet oxidation of various biomasses. Chem Eng J 2015;279:715–24. https://doi.org/10.1016/j.cej.2015.05.086.
[60] Reza MT, Freitas A, Yang X, Coronella CJ. Wet air oxidation of hydrothermal carbonization (HTC) process liquid. ACS Sustainable Chem Eng 2016;4:3250–4. https://doi.org/10.1021/acssuschemeng.6b00292.
[61] Wnukowski M, Owczarek P, Niedźwiecki Ł. Wet torrefaction of miscanthus – characterization of hydrochars in view of handling, storage and combustion properties. J Ecol Eng 2015;16:161–7. https://doi.org/10.12911/22998993/2950.
[62] Yan W, Hastings JT, Acharjee TC, Coronella CJ, Vásquez VR. Mass and energy balances of wet torrefaction of lignocellulosic biomass. Energy Fuel 2010;24:4738–42. https://doi.org/10.1021/ef901273n.
[63] Skřínská M, Skřínský J, Dolníček P, Lukešová P, Přichystalová R, Serafínová C. Bleve - cases, causes, consequences and prevention. Mater Sci Forum 2014;811:91–4. https://doi.org/10.4028/www.scientific.net/MSF.811.91.
[64] Esen M, Yuksel T. Experimental evaluation of using various renewable energy sources for heating a greenhouse. Energy Build 2013;65:340–51. https://doi.org/10.1016/j.enbuild.2013.06.018.
[65] Su B, Lin F, Ma J, Huang S, Wang Y, Zhang X, et al. System integration of multi-grade exploitation of biogas chemical energy driven by solar energy. Energy 2022;241:122857. https://doi.org/10.1016/j.energy.2021.122857.
[66] Tauber J, Parravicini V, Svardal K, Krampe J. Quantifying methane emissions from anaerobic digesters. Water Sci Technol 2019;80:1654–61. https://doi.org/10.2166/wst.2019.415.
[67] Aragón-Briceño CI, Grasham O, Ross AB, Dupont V, Camargo-Valero MA. Hydrothermal carbonization of sewage digestate at wastewater treatment works: influence of solid loading on characteristics of hydrochar, process water and plant energetics. Renew Energy 2020;157:959–73. https://doi.org/10.1016/j.renene.2020.05.021.
[68] Kovacs Z, Samhaber W. Characterization of nanofiltration membranes with uncharged solutes. Membrantechnika 2008;12:22–36.
[69] Luo J, Ding L, Qi B, Jaffrin MY, Wan Y. A two-stage ultrafiltration and nanofiltration process for recycling dairy wastewater. Bioresour Technol 2011;102:7437–42. https://doi.org/10.1016/j.biortech.2011.05.012.
[70] Chen Z, Luo J, Chen X, Hang X, Shen F, Wan Y. Fully recycling dairy wastewater by an integrated isoelectric precipitation–nanofiltration–anaerobic fermentation process. Chem Eng J 2016;283:476–85. https://doi.org/10.1016/j.cej.2015.07.086.
[71] Campbell BSS, Thorpe RBB, Peus D, Lee J. Anaerobic digestion of untreated and treated process water from the hydrothermal carbonisation of spent coffee grounds. Chemosphere 2022;293:133529. https://doi.org/10.1016/j.chemosphere.2022.133529.
[72] Parmar KR, Ross AB. Integration of hydrothermal carbonisation with anaerobic digestion; opportunities for valorisation of digestate. Energies 2019;12:1586. https://doi.org/10.3390/en12091586.
[73] De la Rubia MA, Villamil JA, Rodriguez JJ, Mohedano AF. Effect of inoculum source and initial concentration on the anaerobic digestion of the liquid fraction from hydrothermal carbonisation of sewage sludge. Renew Energy 2018;127:697–704. https://doi.org/10.1016/j.renene.2018.05.002.
[74] Čater M, Zorec M, Marinšek Logar R. Methods for improving anaerobic lignocellulosic substrates degradation for enhanced biogas production. Springer Sci Rev 2014;2:51–61. https://doi.org/10.1007/s40362-014-0019-x.
[75] Detman A, Bucha M, Treu L, Chojnacka A, Pleśniak Ł, Salamon A, et al. Evaluation of acidogenesis products' effect on biogas production performed with metagenomics and isotopic approaches. Biotechnol Biofuels 2021;14:125. https://doi.org/10.1186/s13068-021-01968-0.
[76] Moran EJ, Easterday OD, Oser BL. Acute oral toxicity of selected flavor chemicals. Drug Chem Toxicol 1980;3:249–58. https://doi.org/10.3109/01480548009002221.
[77] Silva-Junior EA, Ruzzini AC, Paludo CR, Nascimento FS, Currie CR, Clardy J, et al. Pyrazines from bacteria and ants: convergent chemistry within an ecological niche. Sci Rep 2018;8:2595. https://doi.org/10.1038/s41598-018-20953-6.
[78] Janssens TKS, Tyc O, Besselink H, de Boer W, Garbeva P. Biological activities associated with the volatile compound 2,5-bis(1-methylethyl)-pyrazine. FEMS Microbiol Lett 2019;366:1–10. https://doi.org/10.1093/femsle/fnz023.
[79] Sertçelik M. Synthesis, spectroscopic properties, crystal structures, DFT studies, and the antibacterial and enzyme inhibitory properties of a complex of Co(II) 3,5-difluorobenzoate with 3-pyridinol. J Chem Res 2021;45:42–8. https://doi.org/10.1177/1747519820924636.
[80] Mikucka W, Zielinska M. Individual phenolic acids in distillery stillage inhibit its biomethanization. Energies 2022;15:5377. https://doi.org/10.3390/en15155377.